



Selection and optimization of pin cross-sections for electronics cooling

N. Sahiti ^{a,*}, F. Durst ^a, P. Geremia ^b^a Institute of Fluid Mechanics, Friedrich-Alexander-University Erlangen-Nuremberg, Cauerstr. 4, D-91058 Erlangen, Germany^b ES.TEC.O. s.r.l., Area Science Park, Padriciano 99, 34012 Trieste, Italy

Received 24 February 2006; accepted 6 May 2006

Available online 10 July 2006

Abstract

Pin fins are widely used as elements that provide increased cooling for electronic devices. Increasing demands regarding the performance of such devices can be observed due to the increasing heat production density of electronic components. For this reason, extensive work is being carried out to select and optimize pin fin elements for increased heat transfer. In the present paper, a procedure is described to select heat exchanger surfaces with pin fins in accordance with their location in a performance diagram. Such a diagram provides performance comparisons of pin fins with respect to two operating parameters: the heat transfer rate per unit base surface area and the power input for the same area. It is shown that elliptical cross-sections offer the best performance compared with all other investigated cross-sections for pin fins. The present work demonstrates that the heat exchanger performance plot allows also the selection of the best elliptical cross-section design within the initial design set (design set obtained numerically) in analogy with the Pareto-optimality approach. However, the real optimal geometry of the elliptical cross-section is deduced from commercial optimization software, modeFRONTIER. It is shown that by subsequent use of the virtual solutions from the response surface modelling (RSM) of that software and their validation with Star-CD, a complete “Pareto-frontier solution” can be obtained.

© 2006 Elsevier Ltd. All rights reserved.

Keywords: Pin fins; Heat transfer rate; Power input; Selection; Optimization**1. Introduction and aim of the work**

One of the primary goals in the design of modern thermal systems for cooling of electronic components is the achievement of more compact and, hence, efficient heat transfer devices. This requires the employment of surfaces with high heat transfer coefficients and high area compactness. Particular attention has to be paid to the selection/design of heat transfer surfaces if the required energy-carrying fluid turns out to be a gas. It is well known that gases have heat transfer coefficients that are about 100 times lower than those of liquids. This is usually compensated with larger heat transfer areas and it is the aim of the work of engineers to have the surface area reduced by enhancing

the heat transfer coefficients. The present paper relates to work in this direction.

To outsiders, the design of efficient heat exchangers appears more like an art than an engineering science. If the designer looks into the literature, finds a number of investigations that relate to the optimization of heat transfer by suitable elements mounted on surfaces. Elements of different shapes and different sizes are used for heat transfer enhancements and the concentration of elements per unit area varies from experiment to experiment. The final results of individual measurements are generalized by plotting the results in the form of Nusselt numbers, Nu , and friction factors, f , as a function of Reynolds numbers, Re . Similar dimensionless numbers, namely Colburn factor, j , and friction factor, f , were employed by Kays and London [1] for presenting heat transfer and pressure drop data. Diagrams of this kind are only useful for scale-up or scale-down investigations, i.e. the same Nusselt number only applies for geometrically similar heat enhancement

* Corresponding author. Tel.: +49 9131 8529481; fax: +49 9131 8529503.

E-mail address: sahiti@lstm.uni-erlangen.de (N. Sahiti).

Nomenclature

A	surface area
a	large elliptical axis
b	small elliptical axis
c_p	isobaric specific heat capacity
d	diameter
e	power input
\dot{m}	mass flow rate
P	pressure
ΔP	pressure drop
\dot{Q}	heat transfer rate
\dot{q}	volume or area reduced heat transfer rate, W/m^3 or W/m^2
Re	Reynolds number
r	elliptical axis ratio
S	pin distance
T	temperature
t	thickness (NACA profile)
U_i	velocity components
U_∞	free stream velocity
\dot{V}	volume flow rate
X	pin distance
x	abscissa (NACA profile)
x_i	Cartesian coordinates
y	ordinate (NACA profile)

Greek symbols

δ_{ij}	Kronecker-delta
η	fan efficiency
ν	kinematic viscosity
ρ	density
τ_{ij}	viscous stress tensor

Subscripts

a	big elliptic axis
b	base surface area reduced parameter, small elliptic axis
f	fluid
h	hydraulic
in	inlet
L	streamwise direction
out	outlet
s	solid
T	transverse direction
t	total
v	volume reduced parameter, constant volume

elements. Hence Nusselt number elements of different shapes or of different number concentration per unit area are not comparable. The Nusselt number of one element can be larger than that of a second element but can still yield lower overall heat transfer when realized in a particular heat exchanger configuration. The appropriate comparison of various elements for heat transfer enhancement should consider their overall performances, namely their heat transfer and pressure drop characteristics. For that purpose Kays and London [1] suggested the plotting of heat transfer coefficient h normalized to unit heat transfer surface area versus pumping power e normalized to the same area. In the study Sahiti et al. [2], that method was for

practical reasons modified by reducing of the heat transfer coefficient to the bare surface area, whereas subsequently [3] it was demonstrated that the most reliable performance prediction can be obtained by comparison of the heat transfer rate per unit heat exchanger volume \dot{q}_v versus the power input per same volume e_v (Fig. 1). Hence heat transfer capability versus effort is plotted, both normalised with the same volume. In this way, elements for heat transfer enhancement that lie higher than others are better in their performance and should be chosen for a particular heat exchanger design. The original data provided by Kays and London [1] were converted by the authors to yield the diagram shown in Fig. 1.

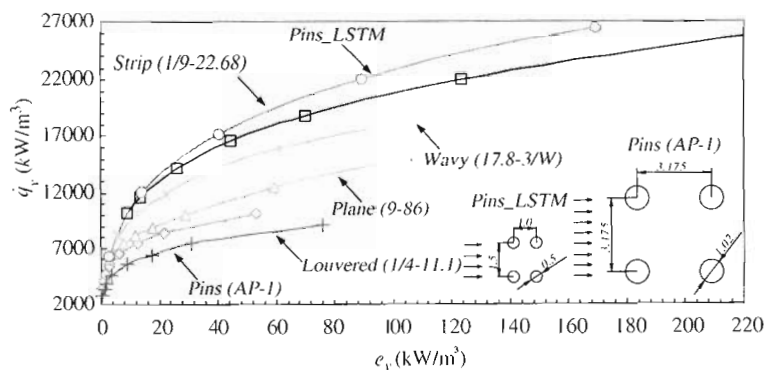


Fig. 1. Performance plot of plate and pin fin heat transfer surfaces.

This diagram clearly indicates that the numerically simulated pin fin configuration *Pins_LSTM* performs better than all other fin forms investigated by Kays and London [1]. For clarity reasons, that kind of comparison in Fig. 1 is shown only for representative fin forms. Fig. 1 also shows that pin fins do not automatically perform better than other fin forms, e.g. the pin configuration AP-1 shows the lowest performance compared with all other fin forms. This is due to the large pin diameter of that configuration and to the large interpin distance (small heat transfer surface compactness). However, providing similar geometric dimensions and heat transfer surface compactness (same order of the magnitude of pin diameter and interpin distance compared with the thickness and distance of other fins), pin fins offer the best performance. Hence, although, in general, pin fins are characterized by higher pressure drops than other fin forms, one can always show that the overall pin fin performance is higher than that of other heat transfer enhancement elements, provided that the appropriate selection of the pin fin geometry is made and also the arrangement on the heat transfer surface is chosen to be optimum. The aim of these studies to obtain the optimum pin fin shape and also the optimum arrangement on the base plate was a major task in these studies. The investigations carried out are summarised here and the final results are presented.

The excellent capabilities of pin fins to enhance the heat transfer rate have been widely identified in the electronics industry but also in other industrial fields. Therefore, different aspects of such elements have been the object of the investigations of numerous workers. Basic research on their heat transfer and pressure drop characteristics were performed by Theoclitus [4], Sparrow and Ramsey [5] and Sara et al. [6]. There have also been some contributions concerning different shapes of pin fin cross-sections which have been applied in electronics cooling but also in other fields of heat transfer. Chen et al. [7] carried out experiments on heat transfer and pressure drop measurements in a rectangular duct with drop-shaped pin fins. They reported the Nusselt number for a channel with drop-shaped pin fins to be slightly higher than those of circular cross-sectional shape. However, they found that, in their experiments, the pressure drop of drop-shaped pin fins was 42–51% less than that of pin fins with circular cross-sections. Li et al. [8] investigated the heat transfer and pressure drop characteristics of elliptical pin fins in a rectangular channel. They measured higher heat transfer coefficient for elliptical fins than those published for circular pin fins. Furthermore, they reported from their experiments a smaller pressure drop for elliptical pins in the range 44–58%.

Regarding the influence of tube spacing on the thermal and fluid dynamic performance of pin fin arrays, valuable information can be derived from works of Bejan et al. [9] and Stanescu et al. [10] in which the authors investigated the optimal tube spacing which would allow the maximum heat transfer within a fixed volume. These works originated the well established geometric optimization method known as “constructal theory”. The optimization according to this

theory is based on the principle of “self optimization” of natural flow systems. The efficiency of the constructal theory in finding the ways of minimum thermal resistance for the heat flow from small-scale electronics components was demonstrated by Bejan [11]. Further analytical and experimental work related to the influence of various pin fin parameters on the performance of heat sinks including the optimal pin spacing was provided by Kobus and Oshio [12] and recently also by Kobus and Oshio [13].

A detail numerical investigation of heat transfer and pressure drop of in-duct flows with pin fin arrays with various cross-sections, for staggered and for inline arrangements, was provided by Sahiti et al. [14]. By presenting heat transfer per unit base surface area versus the input power per unit base surface area, they compared the pin performances for two different geometrical comparison criteria. They demonstrated that from a practical viewpoint, the elliptical cross-section performs better than all other pin cross-sections.

Further aspects of the heat transfer and pressure drop of pin fin arrays e.g. the relative merits of pin fin heat transfer and endwall heat transfer in the overall pin array heat transfer were investigated by VanFossen [15] and Mezger et al. [16].

All this shows that much information is available in the literature on the merits of pin fins for heat transfer enhancement but no final conclusions exist regarding the optimal pin configuration. To remedy this situation, the present authors carried out the study summarized in this paper. The work was carried out with the aim of selecting and optimizing a pin cross-sectional geometry and the arrangements of the pin fins on a heat transfer surface in order to yield the best performance in what might be called an absolute sense. For that purpose, the results and procedure to select the best pin cross-section discussed in detail by Sahiti et al. [14] were applied. Through this, good information resulted, showing that elliptical pin fins with a staggered arrangement gave the best performance. The optimization of that pin configuration carried out in the present work considered the transverse and streamwise pin spacing, the inlet fluid velocity and the elliptical axis ratio.

2. Pin cross-section and geometrical comparison criteria

The identification of the best performing cross-section was done by Sahiti et al. [14] by comparison of the performance of pin fins with cross-sections having a NACA, a drop, a lancet, an elliptical, a circular and a square shape (Fig. 2). As a reference profile was chosen the NACA symmetric profile described by the following equation [17,18]:

$$y = \frac{t}{0.2} (0.2969\sqrt{x} - 0.126x - 0.3516x^2 + 0.2843x^3 - 0.1015x^4) \quad (1)$$

where y denotes the ordinate of the profile, t denotes the maximum profile thickness as a percentage of chord length

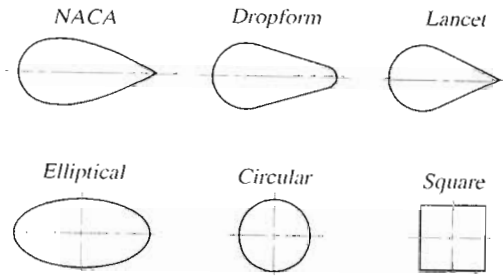


Fig. 2. Cross-sections of pin fins selected for comparison.

and x the abscissa axis coinciding with the chord of the profile. In the present work, the maximum profile thickness was chosen to be 2 mm.

In order to have a NACA profile with realistic manufacturing features, a thickness of 50% of the chord length was chosen, which leads to a chord or profile length of 4 mm. The geometric characteristics of other pin cross-sections were derived based on the hydraulic diameter of the NACA profile and the constraints of the selected geometrical comparison criteria.

In order to provide a fair and physically meaningful basis for the comparison, appropriate geometric comparison criteria which provide similar model dimensions were selected. Furthermore the thermal conditions and fluid properties were similar in order to assess the relative advantages of different pin fin cross-sections. Hence two different geometric criteria were employed. The first comparison criteria (FCC) encompass the same hydraulic diameter d_h , the same coverage ratio ϕ_c and the same pin length l_p .

The second geometric criterion (SCC) was selected from the point of view of the practical application of heat sinks. It provides the same pin blockage area, the same distance between the pins and the same pin length l_p . A more detail explanation of the geometric comparison criteria discussed in the present work was provided by Sahiti et al. [14].

3. Governing equations, simulation notes and prediction procedure

For the simulation of convective heat transfer problems, the governing equations comprise the continuity equation, the momentum equation and the thermal energy equation. The present computations are performed for a three-dimensional laminar flow of air over a heated pin fin array. For steady-state flow and steady-state heat transfer, within a compressible fluid, the governing equations in index notations takes the following form:

- Continuity equation:

$$\frac{\partial(\rho U_i)}{\partial x_i} = 0 \quad (2)$$

- Momentum equation:

$$\rho U_i \frac{\partial U_j}{\partial x_i} = -\frac{\partial P}{\partial x_j} + \frac{\partial \tau_{ij}}{\partial x_i} \quad (3)$$

where for the Newtonian fluids, the momentum transport term, τ_{ij} , reads

$$\tau_{ij} = -\mu \left(\frac{\partial U_i}{\partial x_j} + \frac{\partial U_j}{\partial x_i} \right) + \frac{2}{3} \mu \delta_{ij} \frac{\partial U_k}{\partial x_k} \quad (4)$$

- Thermal energy equation:

$$\rho c_v U_i \frac{\partial T_f}{\partial x_i} = k_f \frac{\partial^2 T_f}{\partial x_i^2} - P \frac{\partial U_i}{\partial x_i} - \tau_{ij} \frac{\partial U_j}{\partial x_i} \quad (5)$$

In the above equations, U_i denotes the velocity components in the Cartesian coordinate system with its coordinates x_i , T_f denotes fluid temperature, P pressure and k_f thermal conductivity of the fluid.

In order to close the set of governing equations in the fluid part, air was considered to behave like an ideal gas and hence the density was considered to be dependent on air temperature and air pressure:

$$\rho = f(T, P) \quad (6)$$

The conjugate heat transfer from pin fin arrays implies the simultaneous solution of Eqs. (2)–(6) and the solid energy equation, which reads

$$\frac{\partial^2 T_s}{\partial x_i^2} = 0 \quad (7)$$

The number of pin rows in the streamwise direction was selected based on Zukauskas [19], who demonstrated that the flow and temperature patterns after 16 rows can be considered fully developed. The flow developing inlet block for the FCC was taken to be $5d_h$, whereas the outlet block length was set equal to $15d_h$ in order to avoid the influence of eventual back flow streams in the final results. For the SCC the length of these blocks was set to $5t_p$ and $15t_p$, respectively, where t_p is the maximum pin thickness projected in the flow direction.

The boundary conditions were selected based on a heat sink model comprising a hot-plate with constant temperature ($=70^\circ\text{C}$), adiabatic side walls, adiabatic top wall. The continuity, momentum and energy equations governing the conjugate heat transfer problem presented here were solved using the commercial code Star-CD (v 3.24). The flow and temperature field was considered to be in the steady-state. The fluid was selected to be air with constant inlet temperature ($=20^\circ\text{C}$). The isobaric specific heat capacity and thermal conductivity of air were considered constant whereas the Sutherland model was selected for molecular viscosity. The solid part of the computation domain (pins) was considered to be aluminum with constant and isotropic properties. The detail description of the boundary conditions, validation procedure, and grid independency check is given in Sahiti [3] and Sahiti et al. [14].

For the performance assessment of the investigated pin fins, the heat exchanger performance plot [3] was used. As the lengths of all pins were taken to be same, the heat transfer and the power input were reduced to unit base surface area instead of unit volume of the heat sink. Hence heat transfer per unit base surface area was calculated as

$$\dot{q}_b = \frac{\dot{Q}_t}{A_b} \tag{8}$$

where \dot{Q}_t is total heat transfer from the base wall and from pins into the fluid. It was calculated as

$$\dot{Q}_t = \dot{m}_f c_{pf} (T_{out} - T_{in}) \tag{9}$$

where \dot{m}_f denotes the fluid mass flow rate, c_{pf} the fluid specific heat at constant pressure and T_{out} and T_{in} the outlet and inlet bulk fluid temperatures, respectively.

The power input per unit base surface area was calculated from the expression

$$e_b = \frac{\dot{V}_f \Delta P_t}{\eta A_b} \tag{10}$$

where \dot{V}_f is the volume flow rate of the fluid, ΔP_t the total pressure drop in the computation domain and η the fan efficiency (arbitrarily taken as 0.8).

4. Selection of the best performing cross-section

The computation procedure described in previous section was followed to perform the relative performance comparison of the discussed pin cross-sections [14]. In contrast, the objective of the present work was to select the best cross-section among those investigated by Sahiti et al. [14] regardless of the arrangement and geometric comparison criteria applied there.

For practical application, this means the selection of the pin cross-section which would allow absolutely the highest heat transfer rate for a given pressure drop and unit base area no matter what their arrangement. Therefore, the selection was performed by plotting of the heat transfer per unit base surface area versus power input per unit base surface area of all investigated cases (Fig. 3). The abbreviations shd and sba in Fig. 3 represent the same hydraulic diameter and same blockage area as characteristic con-

straints related to the FCC and SCC, respectively; st and in denotes the staggered and inline arrangement, respectively.

From the graphical presentation of the results in Fig. 3, one can easily conclude that the highest performance is achieved with pin fins having an elliptical cross-section and a staggered arrangement with characteristics according to the FCC.

5. Optimization concept

After the elliptical cross-section had been found to be the best among all cross-section forms investigated the question that naturally arose was the possibility of optimizing such a cross-section. Optimization can be described as the process of seeking improvements of one or more objectives as a function of several input variables with or without constraints. The objectives are selected according to the nature of the problem or process that has to be optimized. In the present work, this is the maximization of heat transfer per unit base area and minimization of power input per unit base area. Depending on the number of the objectives that have to be optimized, the optimization can be characterised as a single-objective or multi-objective optimization problem. In contrast to single-objective optimization problems, in multi-objective optimization problems such as the present one, the notation of the optimality is not so obvious [20]. It may be a single-point solution (weighted sum approach) or a set of optimal solutions (Pareto-optimality approach). For the weighted sum approach, a multi-objective optimization problem is reduced to a single-objective optimization problem by aggregating of the multiple objectives to a single-objective function. The single-objective function represents the sum of the weighted objective values [21]. The main drawbacks of such a procedure are the deep knowledge of the problem required in order to give an adequate preference or weight to individual objectives, and the impossibility of determining more than one solution for a given set of weights to the objectives. Following the Pareto-optimality approach as in the present work, one is interested in finding a set of optimal solutions. The features of such solutions are such that no objective belonging to the optimal solution can be

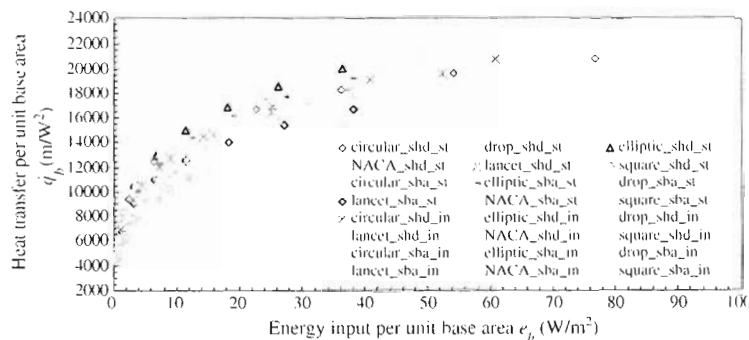


Fig. 3. Absolute performance comparison of pin fin cross-sections.

further improved without deteriorating at least one of the other objectives. Hence such solutions represent a set of compromise solutions obtained by considering all objectives simultaneously. Such solutions are also called non-dominated, in contrast to the dominated solutions which belong to the feasible but not optimal solutions [22]. The set of non-dominated solutions is called the “Pareto-frontier” beyond which no other feasible solution exists.

5.1. Optimization model and initial best performing solution

The design parameters and the objectives of the present optimization model were selected based on the task of the optimization of the elliptical cross-section for pin fins in a staggered arrangement (Fig. 4).

The design parameters are input variables which comprise the variables governing the problem or process to be optimized. In the present work, the following dimensionless groups were selected as input variables:

- Reynolds number: $Re = \frac{U_\infty d_h}{\nu}$,
- transverse pin distance: $X_T = \frac{S_T}{d_h}$,
- streamwise pin distance: $X_L = \frac{S_L}{d_h}$,
- elliptical axis ratio: $r = \frac{b}{a}$,

where d_h is hydraulic diameter of the elliptical cross-section and ν the kinematic viscosity.

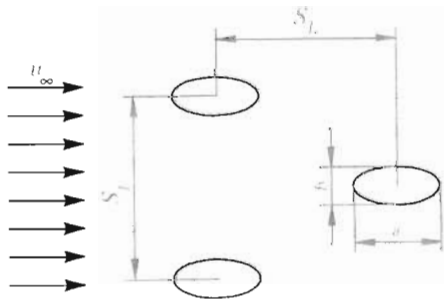


Fig. 4. Elliptical cross-section parameters constituting input optimization variables.

The general mathematical model of the present optimization problem can be formulated as

$$\max[\dot{q}_b = f(Re, X_T, X_L, r)] \tag{11}$$

and

$$\min[e_b = f(Re, X_T, X_L, r)] \tag{12}$$

subject to

$$\left. \begin{aligned} Re_{\min} &\leq Re \leq Re_{\max} \\ X_{T\min} &\leq X_T \leq X_{T\max} \\ X_{L\min} &\leq X_L \leq X_{L\max} \\ r_{\min} &\leq r \leq r_{\max} \end{aligned} \right\} \tag{13}$$

Limiting values of the design parameters constituting constraints (13) were as follows: Re , 180–600; X_T , 1.5–4.5; X_L , 1.5–4.5; and r , 0.2–0.6. In order to obtain an initial set of designs, Re was modified according to inlet velocities from 1.5 m/s to 4 m/s in steps of 0.5 m/s. Dimensionless distances X_T and X_L were modified in steps of 0.5 and the ratio r was modified in steps of 0.1.

The two objectives, \dot{q}_b and e_b , selected for optimization of the elliptical cross-section were used as basic variables also in the heat exchanger performance plot. Hence such a plot may be used in order to obtain the best performing solution within the first (initial set) designs simulated with Star-CD (Fig. 5).

Following the horizontal line passing through the point n , one can see that the lowest power input for the same heat transfer rate is required for the design represented by the curve labeled “sl_d_1.5” (design n). Similarly, following the vertical curve passing through the point n , one can see that the highest heat transfer rate for the same power input is obtained by the design n . The same analysis can be performed for all other designs lying on the curve “sl_d_1.5” which is obtained for $Re = 200$ –530, $X_T = 3.5$, $X_L = 1.5$ and $r = 0.4$. Hence the curve “sl_d_1.5” represents the solution that offers the best performance within the initial set of designs. Such a solution is in analogy with the Pareto-optimality approach in terms of the impossibility of improving an objective without deteriorating the other objectives.

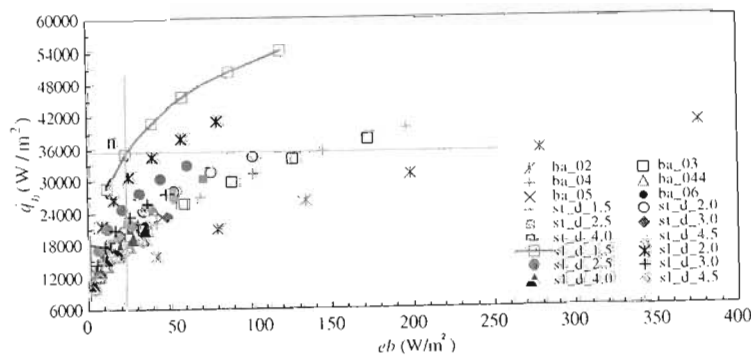


Fig. 5. Best performing solution within the initial designs.

5.2. Pareto-optimality set-up with modeFRONTIER

The best performing solution based on the heat exchanger performance plot was determined based only on the investigated designs. The determination of the full optimal solutions by direct plotting of objectives against each other as in the heat exchanger performance plot would require tedious trial and error simulation procedures. Hence the usual procedure with such tasks is to employ a suitable optimization algorithm to do the job in a much more elegant way. In the present work, the optimization task was performed by using the powerful optimization software modeFRONTIER [23].

In software terms, modeFRONTIER is a general-purpose design tool which enables the designer to search for optimal designs over a number of criteria (e.g. cost, efficiency, weight, volume) within a given design space. The designs generated during optimization make up the trade-off surface (Pareto-frontier). The Pareto-frontier is then

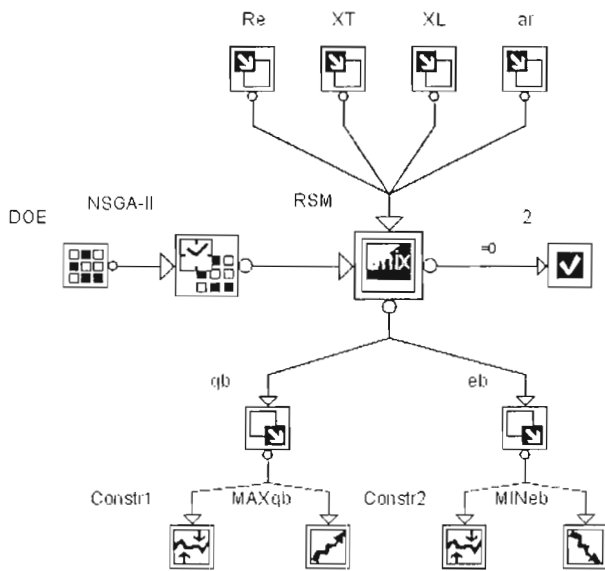


Fig. 6. modeFRONTIER workflow for pin cross-section optimization.

processed by a decision support tool that generates a utility function to suit the designer’s aims best.

5.2.1. Optimization strategy

The initial designs presented in Fig. 5 (108 designs in total) serve as the preliminary design space for modeFRONTIER. Using the Data Wizard Tool, the initial 108 designs are imported into the modeFRONTIER Design Table. With the exception of the optimization algorithm, objectives and constraints, the rest of the optimization scheme (Fig. 6) was automatically generated at the end of that procedure.

As already stated the aim of the present optimization task was the determination of a compromise solution according to the Pareto-optimality approach. The software modeFRONTIER allows the derivation of such a solution starting from the existing Design Table containing the 108 initial designs. The Pareto designs (Fig. 7) obtained from the preliminary exploration represents the most valuable part of the input variable space according to the Pareto dominance definition. Note the same form of the diagrams in Figs. 5 and 7, the only difference being that in Fig. 7 the full Pareto-frontier over the design space was automatically derived and highlighted by modeFRONTIER.

5.2.2. Response surface modeling (RSM) creation and input space exploration

modeFRONTIER is provided with several algorithms designed for data interpolation; the Kriging algorithm was selected because of its good accuracy value on interpolation error over the output variables.

After the RSM has been built for the output variables, it is possible to use the surrogate model to evaluate the performance of pins instead of real solver (Star-CD). Since the design evaluation using RSM is very fast, a massive optimization of the design space is performed by using the response surface (Fig. 8). Thus, virtual optimization is the optimization carried out by running the problem on the surrogate model. The NSGA-II optimization algorithm was used for the present work as it is based on a fast and elitist multi-objective evolutionary algorithm. A fast

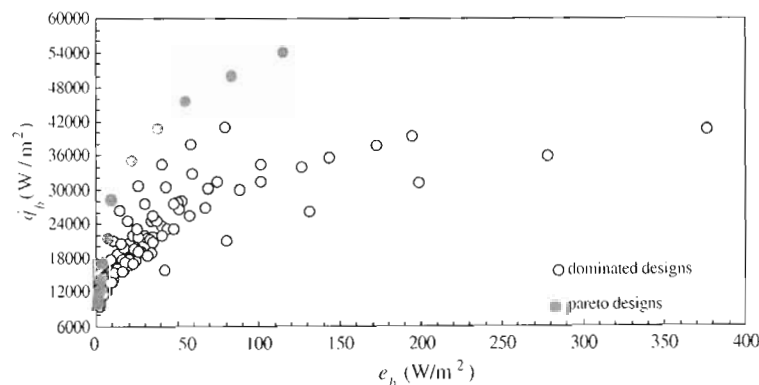


Fig. 7. Preliminary Pareto designs.

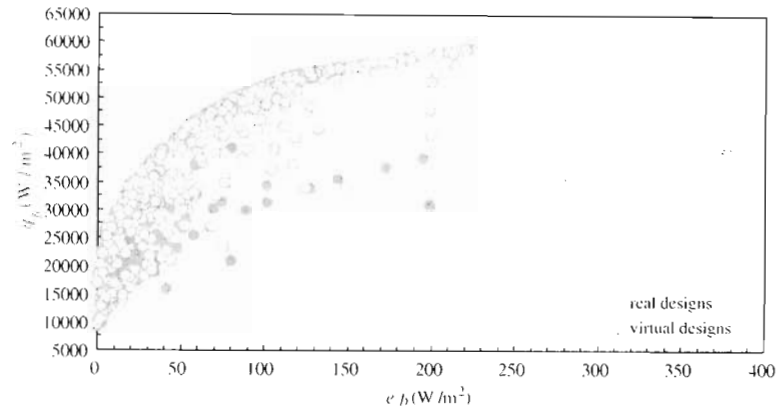


Fig. 8. The use of the RSM allows wide exploration of the domain space.

and clever non-dominated sorting procedure is implemented, in addition to elitism for multi-objective searching, using an elitism-preserving approach. At the end of the virtual optimization, the best so far designs (those belong to the Pareto-frontier) are re-calculated by running the real solver. This process is named validation of the response surface. More precisely, three Pareto points are selected by using Kriging RSM and then evaluated using Star-CD in order to obtain a measure of the interpolation error between real and virtual points. The accuracy of the initial response surface is fairly low; therefore, a new interpolation function is needed. For this purpose, the results given

by the real CFD analysis allow one to update the existing database with three more designs. At this point, a new RSM training is carried out by using Kriging algorithm once again. As a result, a new response surface is created with a reduced interpolation error, compared with the initial one.

A new optimization phase subsequently takes place by using response surface as virtual solver with a genetic algorithm set as scheduler. As previously, three Pareto points are selected and then validated with Star-CD. This recursive task stops once the accuracy level of the response surface becomes acceptable for the designer.

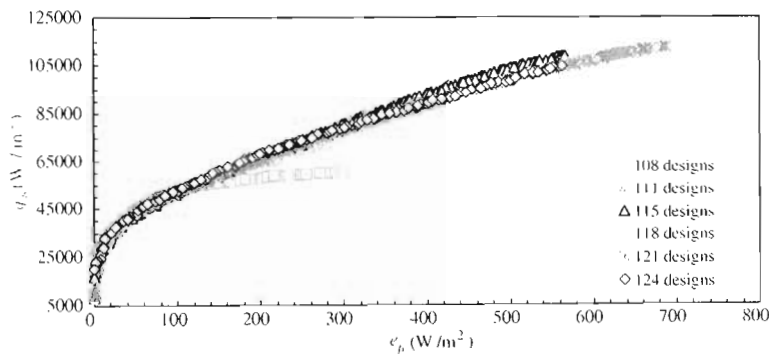


Fig. 9. Pareto-frontier of predicted points according to the response surface.

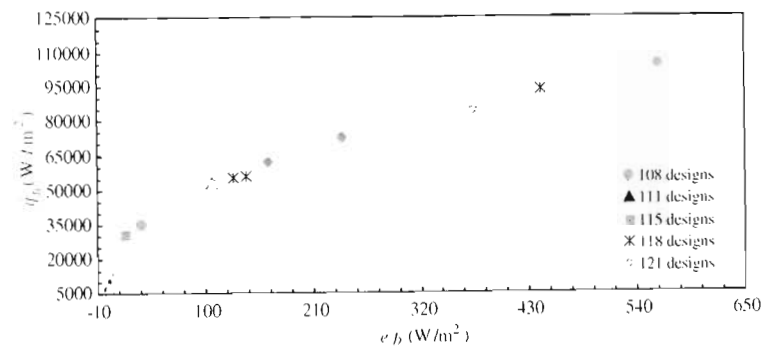


Fig. 10. Pareto-frontier of predicted points after validation with Star-CD.

Following this approach, five consecutive RSM trainings in total are needed so as to reach a sufficient accuracy of the definitive response surface. Once the latter has been built, a very effective tool is available to fulfil the whole Pareto-frontier wherein the best solutions lie.

Fig. 9 depicts the evolution of the Pareto-frontier for each of the five steps of creation of the definitive response surface. Fig. 10 shows the results of the validation of the predicted solutions by response surface for each of the five attempts. It can be seen that all the designs after validation belong to the Pareto-frontier.

6. Conclusions and final remarks

Seeking effective heat transfer methods, different measures have been suggested and employed to increase the heat transfer rate on the side of the heat transfer surface with the largest thermal resistance. Over the years, pin fins have been proved to be the most effective measures for increasing convective heat transfer. Although the utilisation of pin fins in some types of heat exchangers (e.g. in the automobile, air conditioning and aerospace industries) up to now has not been established, pin fins have been widely used in electronic industry. Having in mind the rapid increase in dissipation power of electronic components and the continuing demands on their compactness, the selection of the appropriate pin cross-section and its optimization are of great importance. Hence the major aim of the present work was the demonstration of a simple and practical procedure for selection and optimization of the pin cross-section for electronics cooling. At the beginning of the present paper a brief description of the early work of the authors, related to the comprehensive investigation of pin cross-section in their overall performance, was presented. Based on those results, the selection of the best pin cross-sections no matter what their arrangement was performed. By means of the heat exchanger performance plot, the elliptical cross-section was found to be the best performing cross-section. Subsequently it was demonstrated that the heat exchanger performance plot permits also the determination of the best solutions within the initial investigated designs of that cross-section in analogy with the Pareto-optimality approach. However, the real optimization of the elliptical cross-section was performed using the commercial optimization software modeFRONTIER. It was demonstrated that subsequent estimations of the Pareto solutions based on response surface modeling of modeFRONTIER and their validation with Star-CD converges into a completed Pareto-frontier. In that way, the user can obtain a complete set of optimal solutions by considering the heat transfer and power input per unit base surface area. Since the Pareto-optimality approaches excludes *a priori* giving any weight to the objectives, the described optimization procedure offers the designer complete freedom to choose the most appropriate solution for a particular application from the Pareto-frontier.

References

- [1] W.M. Kays, A.L. London, Compact Heat Exchangers, Krieger, Malabar, 1998.
- [2] N. Sahiti, F. Durst, A. Dewan, Heat transfer enhancement by pin elements. *Int. J. Heat Mass Transfer* 48 (2005) 4738–4747.
- [3] N. Sahiti, Thermal and fluidodynamic performance of pin fin heat transfer surfaces, PhD thesis, Friedrich-Alexander-University Erlangen-Nuremberg, Erlangen, 2006.
- [4] G. Theoclitus, Heat-transfer and flow-friction characteristics on nine pin-fin surfaces. *J. Heat Transfer* (1966) 383–390.
- [5] E.M. Sparrow, J.W. Ramsey, Heat transfer and pressure drop for a staggered wall-attached array of cylinders with tip clearance. *Int. J. Heat Mass Transfer* 21 (1978) 1369–1377.
- [6] O.N. Sara, S. Yapici, M. Yilmaz, Second law analysis of rectangular channels with square pin-fins. *Int. Commun. Heat Mass Transfer* 28 (2001) 617–630.
- [7] Z. Chen, Q. Li, D. Meier, H.-J. Warnecke, Convective heat transfer and pressure loss in rectangular ducts with drop-shaped pin fins. *Heat Mass Transfer* 33 (1997) 219–224.
- [8] Q. Li, Zh. Chen, U. Flechtner, H.-J. Warnecke, Heat transfer and pressure drop characteristics in rectangular channels with elliptic pin fins. *Int. J. Heat Fluid Flow* 19 (1998) 245–250.
- [9] A. Bejan, A.J. Fowler, G. Stanescu, The optimal spacing between horizontal cylinders in a fixed volume cooled by natural convection. *Int. J. Heat Mass Transfer* 38 (1995) 2047–2055.
- [10] G. Stanescu, A.J. Fowler, A. Bejan, The optimal spacing of cylinders in free-stream cross-flow forced convection. *Int. J. Heat Mass Transfer* 39 (1996) 311–317.
- [11] A. Bejan, Constructal theory network of conduction paths for cooling a heat generating volume. *Int. J. Heat Mass Transfer* 40 (1997) 799–811.
- [12] C.J. Kobus, T. Oshio, Development of a theoretical model for predicting the thermal performance characteristics of a vertical pin-fin array heat sink under combined forced and natural convection with impinging flow. *Int. J. Heat Mass Transfer* 48 (2005) 1053–1063.
- [13] C.J. Kobus, T. Oshio, An experimental and theoretical investigation into the thermal performance characteristics of a staggered vertical pin fin array heat sink with assisting mixed convection in external and in-duct flow configurations. *Exp. Heat Transfer* 19 (2006) 129–148.
- [14] N. Sahiti, A. Lemouedda, D. Stojkovic, F. Durst, E. Franz, Performance comparison of pin fin in-duct flow arrays with various pin cross-sections. *Appl. Therm. Eng.* 26 (2006) 1176–1192.
- [15] G.J. VanFossen, Heat-transfer coefficients for staggered arrays of short pin fins. *Trans. ASME* 104 (1982) 268–274.
- [16] D.E. Mezger, C.D. Fan, S.W. Haley, Effects of pin shape and array orientation on heat transfer and pressure loss in pin arrays. *Trans. ASME* 106 (1984) 252–257.
- [17] N.E. Jacobs, Tests of six symmetrical airfoils in the variable density wind tunnel. NACA Report No. 385, NACA, Washington, DC, 1931.
- [18] N.E. Jacobs, K.E., Ward, R.M. Pinkerton, The characteristics of 78 related airfoil sections from tests in the variable-density wind tunnel. NACA Report No. 460, NACA, Washington, DC, 1933.
- [19] A. Zukauskas, *Advances in Heat Transfer*, vol. 18, Academic Press, New York, 1987, pp. 87–159.
- [20] N. Marco, S. Lanteri, J.-A. Desideri, J. Pèriaux, *Evolutionary Algorithms in Engineering and Computer Science*, Wiley, Chichester, 1999, Chapter 22, pp. 445–456.
- [21] E. Zitzler, L. Thiele, An evolutionary algorithm for multiobjective optimization: the strength Pareto approach, TIK-Report, No. 43, TIK, Zürich, 1998.
- [22] C. Poloni, V. Pediroda, *Genetic Algorithms and Evolution Strategies in Engineering and Computer Science, Recent Advances and Industrial Applications*, Wiley, Chichester, 1997, Chapter 13, pp. 267–288.
- [23] ESTECO: modeFRONTIER software, www.esteco.it.

